Subcellular antibiotic visualization reveals a dynamic drug reservoir in infected macrophages

Daniel J. Greenwood[1], **Mariana Silva Dos Santos**[1], **Song Huang**[2], **Matthew R.G. Russell**[1], **Lucy M. Collinson**[1], **James I. MacRae**[1], **Andy West**[3], **Haibo Jiang**[2,4,*], **Maximiliano G. Gutierrez**[1,*]

[1]The Francis Crick Institute, London, UK

[2]Centre for Microscopy, Characterisation and Analysis, University of Western Australia, Perth, AU

[3]GlaxoSmithKline, Stevenage, UK

[4]School of Molecular Sciences, University of Western Australia, Perth, AU

Abstract

Tuberculosis, caused by the intracellular pathogen *Mycobacterium tuberculosis*, remains the world's deadliest infectious disease. Sterilising chemotherapy requires at least six months of multidrug therapy. Difficulty visualising the subcellular localisation of antibiotics in infected host cells means that it is unclear whether antibiotics penetrate into all mycobacteria-containing compartments in the cell. Here, we combine correlated light, electron and ion microscopy to image the distribution of Bedaquiline in infected human macrophages at sub-micrometre resolution. Bedaquiline accumulated primarily in host cell lipid droplets, but heterogeneously in mycobacteria within a variety of intracellular compartments. Furthermore, lipid droplets did not sequester antibiotic but constituted a transferable reservoir that enhanced antibacterial efficacy. Thus, strong lipid binding facilitated drug trafficking by host organelles to an intracellular target during antimicrobial treatment.

Mycobacterium tuberculosis (Mtb) can persist in multiple intracellular niches within human macrophages (1). Given that total host-cell accumulation does not necessarily correlate with antibiotic efficacy against intracellular pathogens, we hypothesised that efficacy is modulated by partitioning of compounds within the host-cell (2). The anti-tubercular antibiotic Bedaquiline is highly lipophilic (3, 4), a trait associated with permeability through tissue at the expense of non-specific binding and host-sequestration (5–7). We tested whether efficacy is linked to the accumulation of the drug in intracellular compartments.

To characterise the intracellular distribution of BDQ, we infected human monocyte-derived macrophages (hMDM) with Mtb for 48 h, giving bacteria time to enter multiple sub-cellular compartments (1). Macrophages were treated with 2.5 mg/L BDQ for 24 h, fixed and imaged by correlative electron microscopy (EM) and ion microscopy (IM) (8) (Fig. S1A). Mtb exhibited a strong ^{31}P signal, likely corresponding to bacterial DNA or polyphosphates. Uninfected macrophages did not have ^{31}P foci outside of the nucleus (Fig. S1B).

BDQ contains a bromine atom, so we determined its localisation by the intensity of the ^{79}Br signal (Fig. 1 A-C). Control macrophages treated with the solvent carrier only did not contain ^{79}Br, confirming the signal was specific (Fig. S1 C). Some ^{79}Br signal will also have derived from primary metabolites of BDQ, which are also active against Mtb (9). BDQ accumulated heterogeneously in Mtb within macrophages, even between neighbouring bacteria (Fig. 1A). BDQ was found in Mtb in a variety of intracellular environments including in a membranous vacuole and a lysing necrotic macrophage (Fig. 1, A and B), a known mycobacterial niche (1).

We also observed Mtb interacting with host lipid droplets (LD) as previously reported (10), and found the LD to be highly enriched with antibiotic (Fig. 1C). No characteristic ion signal exists for LD, so to confirm the organelle identity we stained an infected sample with the neutral lipid dye BODIPY 493/503 and imaged by correlative light, electron and ion microscopy (CLEIM, Fig. 1D). Live-cell imaging prior to fixation showed that the bacteria were intracellular before antibiotic treatment, confirming that the bacteria absorbed BDQ from within the host cell (Movie S1). Liquid chromatography-mass spectrometry (LC-MS) quantification of BDQ from unfixed macrophages treated with pradigastat (11) – an inhibitor of diacyglycerol O-acyltransferase 1 - to inhibit LD formation, or oleate to induce it, confirmed LD as the primary reservoir of intracellular BDQ (Fig. 1E). This validated the CLEIM protocol in preserving the antibiotic distribution during processing.

To determine the relative abundance of BDQ in cellular structures, we normalised the ^{79}Br signal to the cytosolic ^{12}C^{14}N signal (corresponding to protein content) to provide relative quantifications of BDQ enrichment per bacterium. A weak BDQ signal was also detected from other organelles, in particular mitochondria, reflecting reports that BDQ inhibits mammalian ATP synthase (12) (Fig. 1, F-G). A similar distribution of BDQ was observed at a much lower concentration of antibiotic (0.04 mg/L), however at this level the ^{79}Br signal was only marginally detectable (Fig. S1D).

Lipid-laden foamy macrophages are a hallmark of tuberculosis pathogenesis (13). Because LD were the primary site of BDQ accumulation in the host, we investgated the interactions between LD and Mtb in human macrophages. As expected, Mtb exposure induced host LD proliferation (10, 14, 15), even in uninfected "bystander" macrophages (Fig. 2A, S2A). LC-MS analysis found 123 triacylglycerides (TAGs), together with two cholesterol esters and four ceramides, were more abundant in infected macrophages. This included many TAGs containing odd-chain fatty acids, associated with Mtb virulence (16) (Fig. 2B, S3). Confocal microscopy revealed extreme heterogeneity in both bacterial and LD burdens (Fig. 2C). Because intracellular mycobacteria consume host LD as a carbon source (17, 18), we investigated the temporal progression of LD induction and consumption. Live-cell imaging

showed that, as Mtb grows intracellularly, LD proliferation outweighed consumption for the first ~48 h of infection, before consumption eventually reduced the amount of LD (Fig. 2D, S2, D and E, Movies S2 and S3).

Transmission-EM (TEM) showed extensive physical contacts between LD and Mtb or tight Mtb-containing vacuoles (Fig. S2C). We also found that the LD surface protein Perilipin 2 (PLIN2), known to associate with intracellular *M. marinum* (19), labelled 3.8% of Mtb 96 h after infection (95% CI 1.86-6.59, n = 4 donors) (Fig. 2 E). These variable levels of interaction may have contributed to heterogeneity of BDQ accumulation. Mtb secretes lipases (20, 21) and we hypothesised that proximity between LD and Mtb caused degradation of LD. Indeed, some LD in contact with Mtb shrunk over time whereas LD in other parts of the cell remained the same diameter (Fig. 2F, Movie S4).

We next asked whether LD sequestered or transferred BDQ to Mtb. We pre-loaded macrophages with antibiotic and then infected with Mtb. The distribution of BDQ was indistinguishable from samples treated after infection (Fig. 3, A and B). Thus, BDQ can be transferred from a host reservoir to Mtb. Co-treatment with pradigastat – which reduces LD levels - significantly reduced BDQ abundance in Mtb and inhibited pre-loading (Fig. S2B, Fig. 3, A and B). Thus, LD accumulate a BDQ pool that can be transferred to bacteria, although they are not absolutely required for BDQ access to Mtb. The induction of LD formation by the addition of the fatty acid oleate did not prevent BDQ transfer to Mtb (Fig. 3, A and B). Thus, LD may act more as an accessible reservoir than a sequestrator of BDQ.

Damage to the phagosomal membrane and escape into the cytosol is an important feature of Mtb virulence (22). Therefore, we compared macrophages infected with Mtb wild-type and the RD1 strain, which lacks the ESX-1 type VII secretion system required for cytosolic access (Fig. 3C). Both strains showed a similar BDQ signal. Thus, BDQ can be transferred to phagosomal bacteria. Furthermore, we infected macrophages with formaldehyde-killed Mtb to test whether BDQ uptake was actively controlled by bacteria. Killed bacteria showed a non-statistically significant upward trend in BDQ signal (Fig. 3D). We also treated macrophages with the proposed efflux-pump inhibitor verapamil (23), which slightly reduced BDQ accumulation, however its mechanism of action has recently been called into question (24) (Fig. 3D).

Although LD were not essential for BDQ transfer to Mtb, we hypothesised that LD may enhance antibiotic efficacy. In this case, BDQ will accumulate over time in the host macrophage LD, increasing the effective BDQ dose for bacteria that later consume LD. To study marginal changes in BDQ efficacy, we developed two intracellular antibiotic activity assays in which Mtb replication was measured by high-content confocal microscopy (Fig. S4A). BDQ concentrations were selected based on their ability to partially limit Mtb growth (Fig. S4, B and C). Inhibitors targeting lipid-metabolism enzymes, as well as low-density lipoproteins (LDL), were screened for their ability to modulate macrophage lipid droplet burden. Only DGAT-1 inhibitors and oleate were found to be effective and non-toxic. (Fig. S4, D-H). A multiplicity of infection of 1 was used to avoid host-cell necrosis, which would expose Mtb to extracellular BDQ.

Inhibition of LD formation by pradigastat, A922500 and T863 reduced antibiotic efficacy in macrophages treated with 2.5 mg/L BDQ, whereas induction with oleate significantly increased BDQ efficacy (Fig. 4, A and B). Thus, LD facilitated antibiotic effectiveness. Pre-loading of macrophages with BDQ prior to infection results in a similar level of inhibition, indicating an accessible intracellular BDQ reservoir (Fig. 4, A and C). BDQ has a physiological terminal half-life of 6 months (25). Thus, BDQ stored in LD may be accessible well after the patient has stopped treatment. Furthermore, oleate-induction of LD enhanced the efficacy of pre-loaded BDQ at a marginally effective concentration (0.25 mg/L), arguing that these macrophages contained a larger antibiotic reservoir. Conversely, pre-treatment with pradigastat reduced efficacy of 2.5 mg/L BDQ. Separating macrophages by LD and Mtb burden at the single-cell level, we observed that BDQ disproportionately depleted the high-LD/high-Mtb sub-population compared with low-LD/high-Mtb macrophages (Fig. S4I). This pattern held when the LD burden in the population was skewed with oleate or DGAT-1 inhibitors. Thus, BDQ selectively targets Mtb in foamy macrophages.

We propose a new model for the transfer of lipophilic antibiotics to intracellular pathogens, where drugs accumulate in LD and are transferred to the pathogen as LD are consumed. Many intracellular pathogens interact with host LD (26), and we hope that these results will inspire a re-evaluation of the parameters used to screen drug candidates and the importance of sub-cellular pharmacokinetics to understanding antibiotic efficacy.

Supplementary Material

Refer to Web version on PubMed Central for supplementary material.

Acknowledgments

References

1. Lerner TR, et al. J Cell Biol. 2017

2. Carryn S, Van Bambeke F, Mingeot-Leclercq M-P, Tulkens PM. Antimicrob Agents Chemother. 2002; 46:2095–2103. [PubMed: 12069960]

3. Andries K, et al. Science. 2005; 307:223–7. [PubMed: 15591164]

4. Tong AST, et al. ACS Med Chem Lett. 2017; 8:1019–1024. [PubMed: 29057044]

5. Waring MJ. Expert Opin Drug Discov. 2010; 5:235–248. [PubMed: 22823020]

6. Prideaux B, et al. Nat Med. 2015; 21:1223–7. [PubMed: 26343800]

7. Irwin SM, et al. ACS Infect Dis. 2016; 2:251–267. [PubMed: 27227164]

8. Jiang H, et al. Methods. 2014; 68:317–24. [PubMed: 24556558]

9. Liu K, et al. Drug Metab Dispos. 2014; 42:863–866. [PubMed: 24513655]

10. Peyron P, et al. PLoS Pathog. 2008; 4:e1000204. [PubMed: 19002241]

11. Birch AM, Buckett LK, Turnbull AV. Curr Opin Drug Discov Devel. 2010; 13:489–96.

12. Fiorillo M, et al. Aging. 2016; 8:1593–607. [PubMed: 27344270]

13. Russell DG, Cardona P-J, Kim M-J, Allain S, Altare F. Nat Immunol. 2009; 10:943–948. [PubMed: 19692995]

14. Mahajan S, et al. J Immunol. 2012; 188:5593–5603. [PubMed: 22544925]

15. Barisch C, et al. PLOS Pathog. 2017; 13:e1006095. [PubMed: 28103313]

16. Jain M, et al. Proc Natl Acad Sci U S A. 2007; 104:5133–8. [PubMed: 17360366]

17. Daniel J, Maamar H, Deb C, Sirakova TD, Kolattukudy PE. PLoS Pathog. 2011; 7:e1002093. [PubMed: 21731490]

18. Marrero J, Rhee KY, Schnappinger D, Pethe K, Ehrt S. Proc Natl Acad Sci U S A. 2010; 107:9819–24. [PubMed: 20439709]

19. Barisch C, Paschke P, Hagedorn M, Maniak M, Soldati T. Cell Microbiol. 2015; 17:1332–1349. [PubMed: 25772333]

20. Singh KH, et al. J Biol Chem. 2017; 292:11326–11335. [PubMed: 28515317]

21. Daleke MH, et al. J Biol Chem. 2011; 286:19024–34. [PubMed: 21471225]

22. van der Wel N, et al. Cell. 2007; 129:1287–98. [PubMed: 17604718]

23. Adams KN, Szumowski JD, Ramakrishnan L. J Infect Dis. 2014; 210:456–466. [PubMed: 24532601]

24. Chen C, et al. Antimicrob Agents Chemother.

25. van Heeswijk RPG, Dannemann B, Hoetelmans RMW. J Antimicrob Chemother. 2014; 69:2310–2318. [PubMed: 24860154]

26. Melo RCN, Dvorak AM. PLoS Pathog. 2012; 8:e1002729. [PubMed: 22792061]

27. Lerner TR, et al. J Clin Invest. 2016; 126:1093–108. [PubMed: 26901813]

28. Listenberger LL, Brown DA, Listenberger LL, Brown DA. Current Protocols in Cell Biology. Chapter 24:Unit 24.2.

29. Koelmel JP, et al. BMC Bioinformatics. 2017; 18:331. [PubMed: 28693421]

30. Alffenaar J-WC, et al. Antimicrob Agents Chemother. 2015; 59:5675–80. [PubMed: 26149993]

31. Russell MRG, et al. J Cell Sci. 2017; 130:278–291. [PubMed: 27445312]

32. Amiar S, et al. PLOS Pathog. 2016; 12:e1005765. [PubMed: 27490259]

One Sentence Summary

Macrophage lipid droplets accumulate a reservoir of lipophilic antibiotic that is transferred to intracellular *Mycobacterium tuberculosis* during infection.
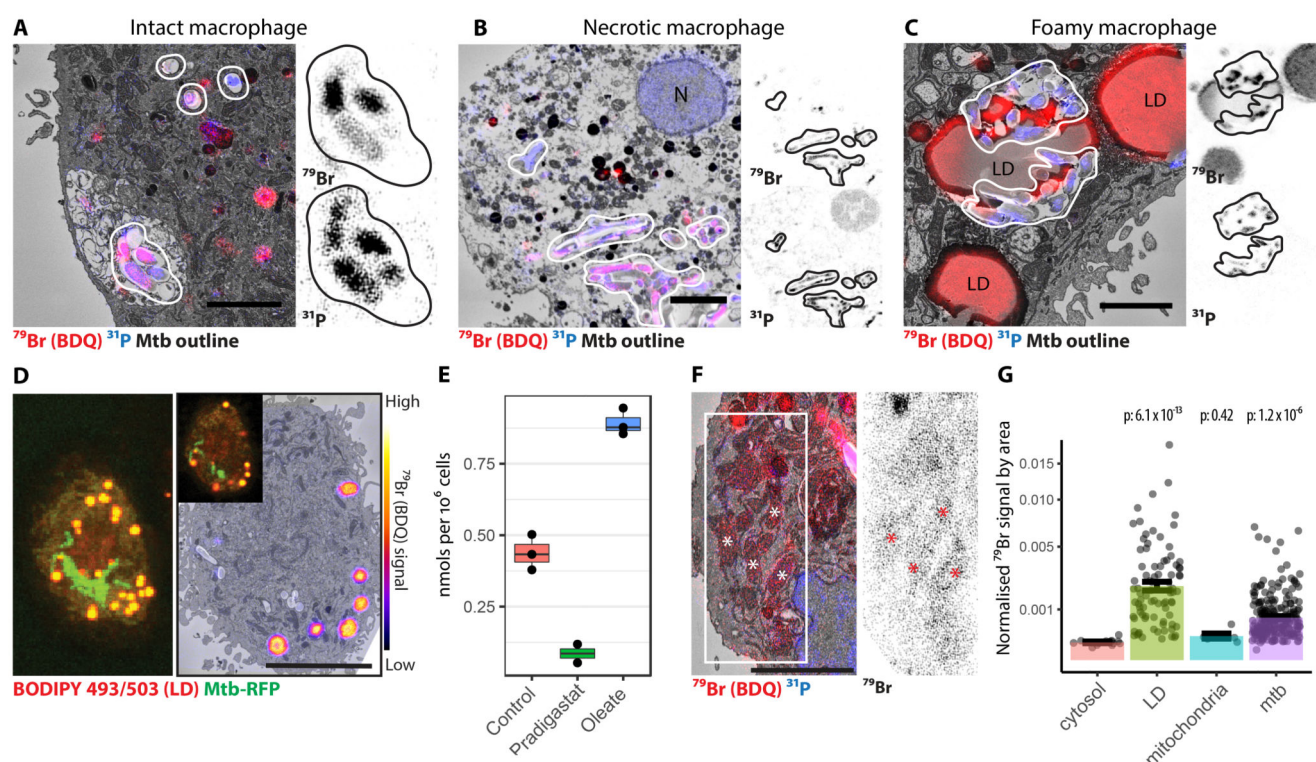
Fig. 1. Bedaquiline accumulated in host LD and Mtb.

(**A-C**) Mtb-infected hMDM, treated with 2.5 mg/L BDQ. EM overlaid with ^{79}Br and ^{31}P signals. Scale: 2 μm. (**D**) (Left) Maximum projection of macrophage infected with Mtb-RFP, treated with 2.5 mg/L BDQ. LD stained with BODIPY appear yellow due to spectral overlap. (Right) LD staining and ^{79}Br signal on EM. Scale: 5 μm. (**E**) BDQ in macrophages treated with 2.5 mg/L BDQ. Data shows means from 4-6 technical replicates from 2-3 donors. (**F**) EM with ^{79}Br signal on mitochondria, starred. Scale: 2 μm. (**G**) Normalised ^{79}Br (BDQ) signal by area. Data shows mean intensity per object, 3 biological replicates, S.E., p-values from Wilcox test, n=6-221. Y-axis square-root scaled.
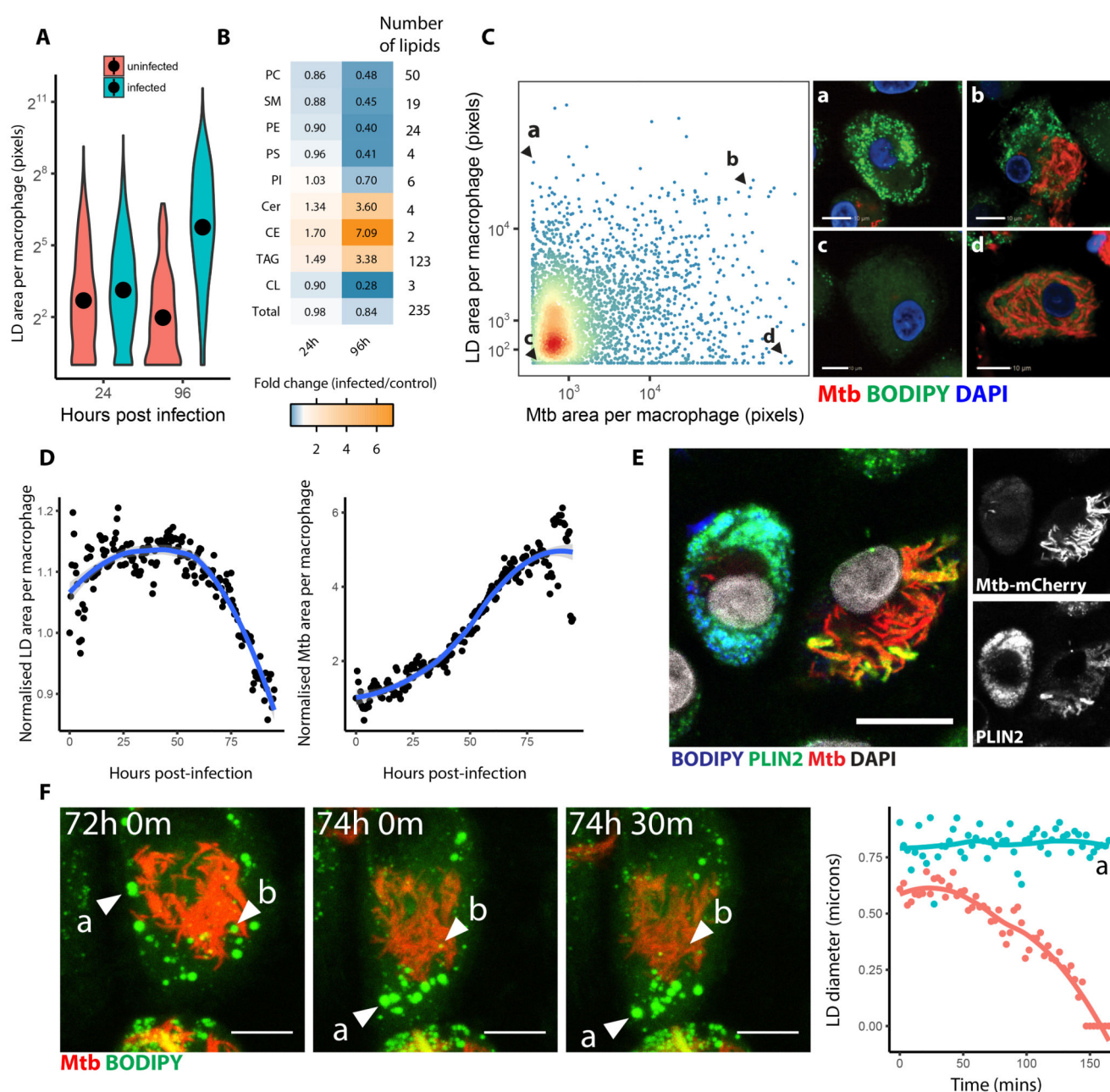
Fig. 2. Mtb induced host LD accumulation and consumption in hMDM.
(**A**) LD area per macrophage, dots show means. (**B**) Fold-changes of significantly (p<0.05) altered lipids relative to uninfected control, n=6 technical replicates. (**C**) Mtb vs LD area 96 h post infection. Axes square root scaled. Scale: 10 μm. (**D**) Mean LD and Mtb burden measured by area, averaged from 38 infected macrophages. LD normalised to uninfected average, starting point of 1. Curve LOESS fitted with 95% confidence interval. (**E**) Mtb infected hMDM stained anti-PLIN2 antibody. (**F**) Maximum-projection from live-cell video of Mtb infected macrophages with LD diameter, right.
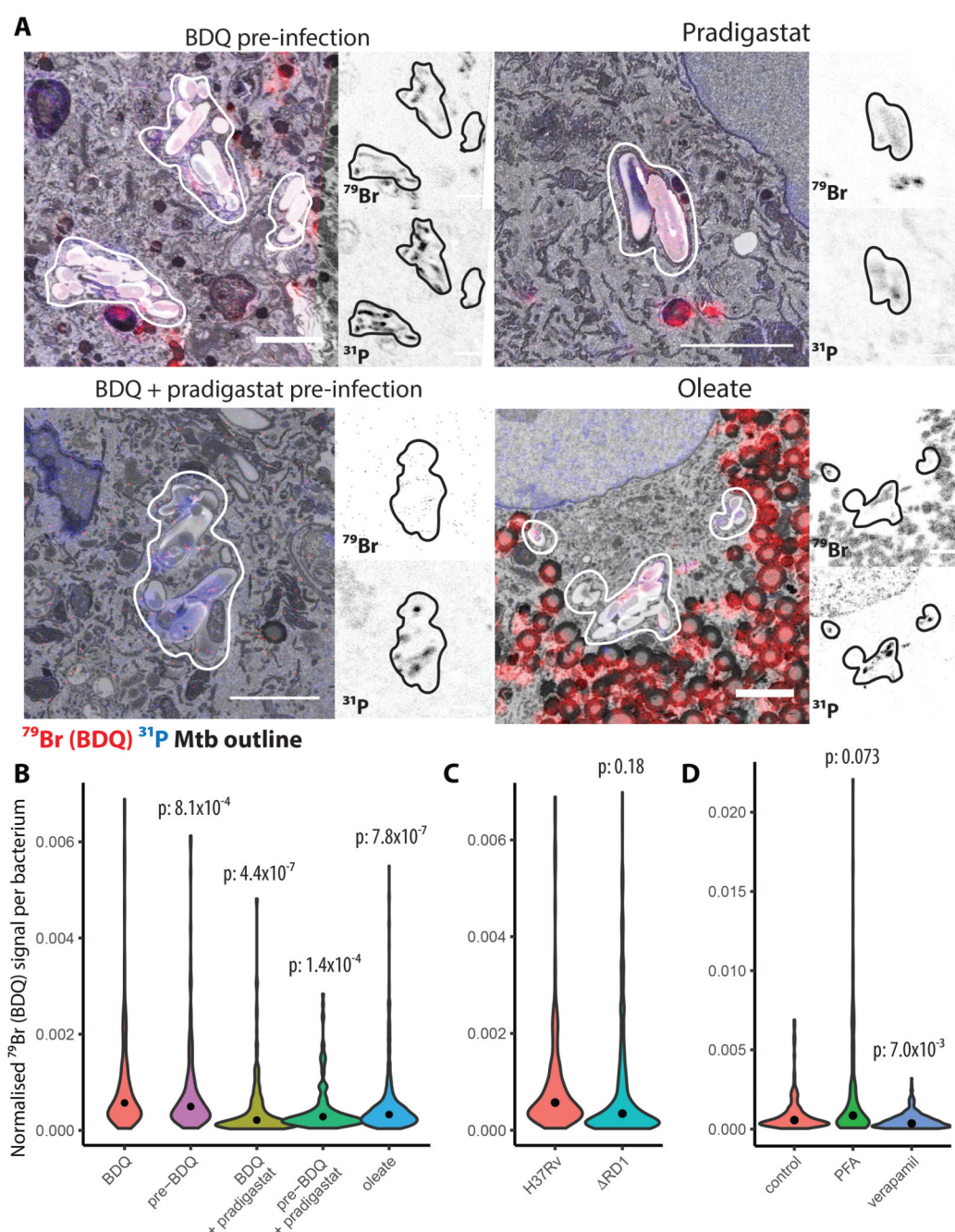
Fig. 3. BDQ was transferred from host LD to Mtb.
(**A**) (Top-left) hMDM treated with 2.5 mg/L BDQ for 24 h, then infected for 24 h; (top-right) 10 mg/L pradigastat during 48 h infection, then 24 h treatment with pradigastat and 2.5 mg/L BDQ; (bottom-left) 2.5 mg/L BDQ and 10 mg/L pradigastat for 24 h prior to infection for 24 h; (bottom-right) 400 μM oleate, followed by 48 h infection and 24 h treatment with 2.5 mg/L BDQ. (**B**) Quantification of (A). Data shows mean signal from 187-640 bacteria per condition, 3 biological replicates, p-values from linear regression. (**C**) ^{79}Br signal from hMDM infected and treated with 2.5 mg/L BDQ for 24 h. P-values as in

(B), 221–643 bacteria analysed per condition, 3 biological replicates. (**D**) ^{79}Br signal from hMDM infected and treated with 2.5 mg/L BDQ for 24 h. In 'PFA', macrophages infected with pre-killed Mtb or 40 mg/L verapamil added with BDQ. P-values as in B, 221–350 bacteria analysed per condition, 3 biological replicates.
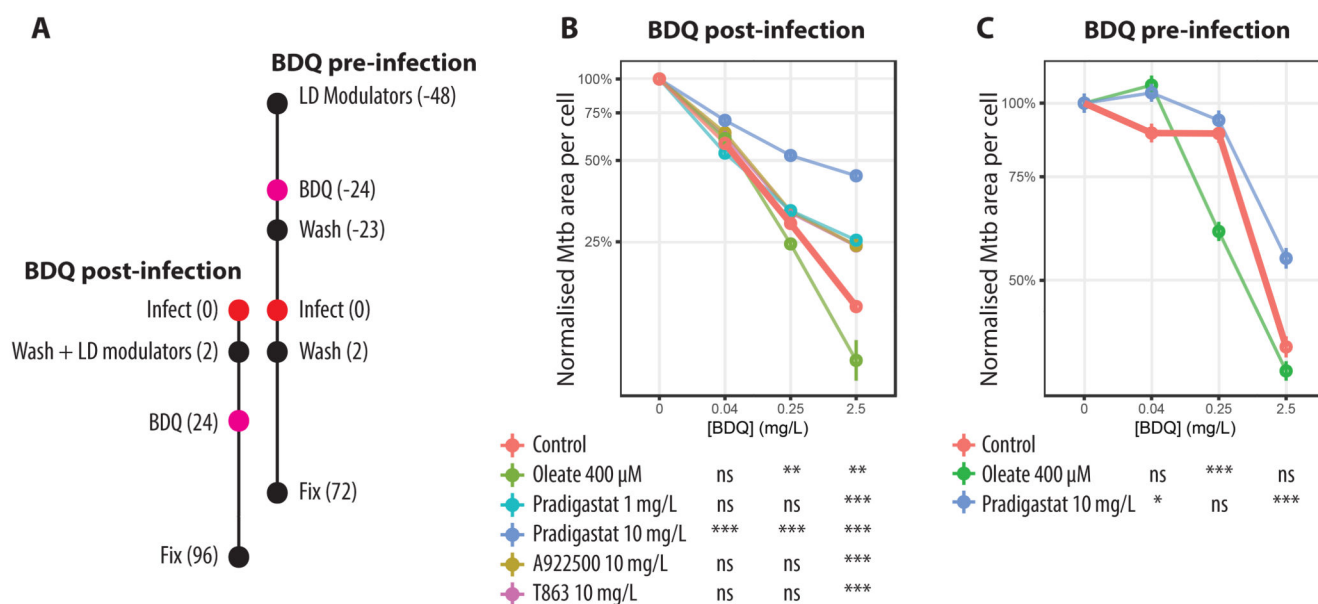
Fig. 4. LD enhanced BDQ efficacy against intracellular Mtb.
(**A**) Experimental timelines, hours in brackets. (**B**) Bacterial area per macrophage at 96 h normalised to BDQ-untreated control for each condition. Data shown are means, S.E.M. from 12937-17180 infected macrophages per LD modulator from 3 donors, p-values from linear regression. Y-axis log-scaled. A922500 overlaps with T863. Significance-codes: '***'<0.001, '**'<0.01, '*'<0.05. (**C**) Bacterial area normalised to BDQ-untreated control. P-values as in **B**, 38795–48466 infected macrophages analysed per LD modulator, 5 monocyte donors. Y-axis log-scaled.